Salvador Garcia Muñoz, Carl Laird, Matthew Realff (Eds.)
Proceedings of the 9th International Conference on Foundations of Computer-Aided Process Design
July 14th to 18th, 2019, Copper Mountain, Colorado, USA.
http://dx.doi.org/10.1016/B978-0-12-818597-1.50075-8

MATERIAL PROPERTY GOALS TO ENABLE CONTINUOUS DIAFILTRATION MEMBRANE CASCADES FOR LITHIUM-ION BATTERY RECYCLING

Elvis A. Eugene, William A. Phillip, and Alexander W. Dowling*
University of Notre Dame
Notre Dame, IN 46556

Abstract

Diafiltration is a continuous operating strategy for staged-membrane cascades, wherein dialysate is strategically added to offset concentration effects and achieve recovery of high purity and high value products. Although common for niche separations in industry, few studies have systematically analyzed multi-stage diafiltration processes. In this paper, we present a novel modeling and superstructure optimization framework 1) to elucidate optimal multi-stage process configurations with complex recycle strategies and 2) to systematically identify property targets for membrane materials. As an illustrative example, we consider the separation of lithium and cobalt ions for battery recycling. We find that if a 3-stage diafiltration process is carefully designed, emerging membrane materials are likely to outperform existing technologies for Li/Co separation in battery recycling. Finally, we discuss planned extensions of the proposed work into a full molecules-to-systems framework for integrated molecular engineering of new materials for targeted separation processes.

Keywords

superstructure optimization, block polymer membrane, staged separation, diafiltration, inverse material design, process intensification

Introduction

Diafiltration processes are common in the food and beverage, pharmaceutical industries (Lipnizki et. al., 2002) as an operating mode for membrane cascades for the recovery of high purity and high value products. It involves the addition of dilute solvent, known as the dialysate, to the feed side of a membrane to offset concentration effects as solvent permeates across the membrane. This allows more of the smaller molecular size solute to permeate through, resulting in a high purity retentate (Cheryan, 1998, Mulder, 1998, Strathmann, 2011). Continuous diafiltration was introduced as a novel concept by Madsen (2001). Nambiar et. al., (2018) demonstrated process feasibility for 400-fold removal of microsolute impurities from protein feed using a two-stage continuous countercurrent diafiltration system. Nevertheless, there is a lack of systematic frameworks to quickly and efficiently design continuous multi-stage diafiltration membrane cascade systems. There also exists a need to find the most promising applications for continuous membrane cascades.

We propose a superstructure-based optimization framework for binary separation via continuous, multi-stage diafiltration. Superstructure optimization is a well-

* To whom all correspondence should be addressed. Email: adowling@nd.edu

established technique to rigorously search a set of process alternatives, i.e. system configurations, to minimize a well-defined objective. See Chen and Grossman (2017), Cremaschi (2015), and Tian et. al. (2018) for recent reviews. The three major steps are: 1) postulate a superstructure representation that encodes all possible (or reasonable) interconnections of flow streams between units in the process networks; 2) define a mathematical model, which often includes mass and energy balances, physical property predictions, transport rates, equipment efficiencies, and costs. Often these models are highly nonlinear, include discrete decisions, and are nonconvex; and 3) select an appropriate computational algorithm and solve the optimization problem to identify the optimum process network configuration. In contrast to simulation techniques, superstructure optimization explicitly manipulates configuration parameters such as recycle strategies, split fractions, and the number of stages, and thus exploits many more degrees of freedom to search for novel system configurations. Superstructure optimization has been used to design optimum membrane network configurations for gas permeation systems (Uppaluri et. al., 2004, Uppaluri et. al., 2006) and reverse osmosis (RO) based water purification systems (Khor et. al., 2011, Sassi and Mujtaba, 2013, Alnouri and Linke, 2014, Saif and Almansoori, 2015, Du et. al., 2015, Kotb, et. al., 2016, Du et. al., 2016). For example, Du et. al., (2016) used superstructure optimization to develop a novel permeate-split design for RO networks which enabled a 0.67 – 6.82 % reduction in unit production cost of water and 3.28 – 7.61 % energy savings compared to conventional designs. This is one of several examples were superstructure optimization helped discover novel system configurations to achieve specific improved separation outcomes.

As a demonstration case study, we consider continuous diafiltration cascades with polymer membranes to recover cobalt (Co) and lithium (Li) from spent lithium ion batteries (LIBs). The current worldwide production of Co and Li does not match the demand caused by the rapid growth of LIBs used in electronic devices and vehicles (Lv et. al. 2018), necessitating the secondary recovery of these metals from spent batteries. The most commonly employed process for the extraction of cathodic materials from spent LIBs is acid leaching followed by solvent extraction, wherein the efficiency of the process increases with the strength of the solvents (e.g., lower pH) used (Zeng et. al., 2014). We propose to mitigate the hazards associated with such a process by designing novel polymer membrane-based diafiltration separations to recover metal rich buffer solutions that can be further processed to generate high purity metals. These membranes have several properties that can be tuned at a molecular level (Mulvena et. al., 2014) to control the permeability of Li relative to Co. For this application, we consider two questions:

1. How do the tradeoffs between purity and recovery in a diafiltration cascade depend on the number of stages?
2. What membrane material performance levels would make diafiltration a disruptive technology for LIB recycling?

Mathematical Model

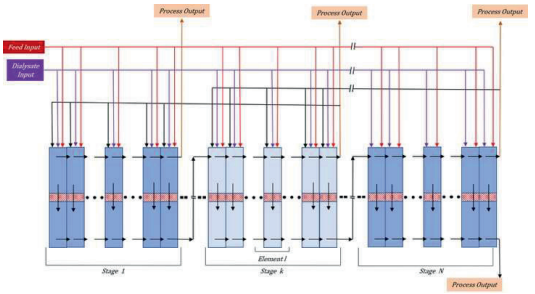

Figure 1: Superstructure for LIB recycling using continuous diafiltration membrane cascade. The red box indicates the fresh feed input to the system (model parameter $\boldsymbol{Q_{ff}}$) which is split into individual flow streams across the cascade (model variables $\boldsymbol{q_{ff,k,l}}$), shown by the red arrows. The purple box indicates the fresh dialysate input to the system (model parameter $\boldsymbol{Q_{fd}}$) which is split into individual flow streams across the cascade (model variables $\boldsymbol{q_{fd,k,l}}$), shown by the purple arrows. Black arrows indicate recycled retentate to the immediately preceding stage (model variables $\boldsymbol{q_{re,k,l}}$). Orange arrows in the top half of the figure are the retentate side products (model variables $\boldsymbol{q_{pr,k,l}}$) while the single orange arrow at the bottom of the figure is the permeate product (model variable $\boldsymbol{q_{p,N,M}}$). Subscripts $\boldsymbol{k}$ and $\boldsymbol{l}$ respectively indicate the stage and element to which the stream is flowing, where the total number of stages is $\boldsymbol{N}$ and the total number of elements per stage is $\boldsymbol{M}$.

To address these questions, we pose a superstructure for the continuous diafiltration membrane cascade, as shown in Figure 1. It consists of *N* staged membrane units with interconnecting streams and each stage is discretized into *M* finite elements. The streams mix only inside the membrane elements. System inputs of feed and dialysate can be injected at any point (element) in the cascade. Retentate can be withdrawn from the end of any stage and can be split into product and recycle streams. Recycle is admitted into only the immediately preceding stage (black arrows), but can be admitted to any location on the feed side. The retentate side product will be enriched in solute for which the membrane is less permeable. Cascading is realized by allowing the permeate at the end of one stage to enter as feed into the next. The permeate at the end of the last stage is withdrawn as product. It is rich is the more permeable solute. For the LIB recycling case study, we considered a charged membrane which was more selective to the monovalent solute, making the permeate enriched in Li while the retentate becomes enriched in Co. We highlight that this superstructure encodes all reasonable recycle

strategies for dialysate including those already experimentally demonstrated.

Each membrane stage and flow stream interconnections are modeled as follows:

Sets:
$\mathcal{I} = \{1, 2, \dots O\}$ (solutes)
$\mathcal{J} = \{ff, fd, rd, sf, f, r, fl, p, pr, re\}$
(all flow streams)
$\mathcal{J}_1 = \{ff, fd, rd, sf, f, r, fl, p\} \subset \mathcal{J}$
(inlet streams)
$\mathcal{J}_2 = \{pr, re\} \subset \mathcal{J}$ (retentate side stage outlets)
$\mathcal{J}_3 = \{ff, fd, rd, sf\} \subset \mathcal{J}_1$ (feed side inlets)
$\mathcal{J}_4 = \{r, fl\} \subset \mathcal{J}_1$ (element outlets)
$\mathcal{J}_5 = \{ff, fd\} \subset \mathcal{J}_1$ (system inlets)
$\mathcal{K} = \{1, 2, \dots N\}$ (stages)
$\mathcal{L} = \{1, 2, \dots M\}$ (elements)

$\mathcal{I}$ is the set of all the solutes in the system. In the LIB case study, $\mathcal{I} = \{1, 2\}$ where solute 1 is Li and solute 2 is Co. $\mathcal{J}$ contains the different flow streams modeled – *ff*: fresh feed, *fd*: fresh dialysate, *rd*: recycled dialysate, *sf*: secondary feed, *f*: element feed, *r*: retentate, *fl*: flux across membrane, *p*: permeate, *pr*: retentate product, *re*: recycled retentate. $\mathcal{J}_3$to $\mathcal{J}_5$ are subsets of $\mathcal{J}_1$. $\mathcal{K}$ and $\mathcal{L}$ denote the stages and elements, respectively.

Material balances:

$$\sum_j q_{j,k,l} = Q_j \; \forall j \in \mathcal{J}_5, k \in \mathcal{K}, l \in \mathcal{L} \quad (1)$$

$$q_{j,k,l} \leq Q_j \forall j \in \mathcal{J}_5, k \in \mathcal{K}, l \in \mathcal{L} \quad (2)$$

$$c_{i,j,k,l} = C_{i,j} \; \forall i \in \mathcal{I}, j \in \mathcal{J}_5, k \in \mathcal{K}, l \in \mathcal{L} \quad (3)$$

$$\sum_j q_{j,k,l} = q_{f,k,l} \; \forall j \in \mathcal{J}_3, k \in \mathcal{K}, l \in \mathcal{L} \quad (4)$$

$$\sum_j q_{j,k,l} \times c_{i,j,k,l} = q_{f,k,l} \times c_{i,f,k,l} \quad (5)$$
$$\forall i \in \mathcal{I}, j \in \mathcal{J}_3, k \in \mathcal{K}, l \in \mathcal{L}$$

$$\sum_j q_{j,k,l} = q_{f,k,l} \forall j \in \mathcal{J}_4, k \in \mathcal{K}, l \in \mathcal{L} \quad (6)$$

$$\sum_j q_{j,k,l} \times c_{i,j,k,l} = q_{f,k,l} \times c_{i,f,k,l} \quad (7)$$
$$\forall i \in \mathcal{I}, j \in \mathcal{J}_4, k \in \mathcal{K}, l \in \mathcal{L}$$

$$\sum_j q_{j,k,M} = q_{r,k,M} \; \forall j \in \mathcal{J}_2 \quad (8)$$

$$c_{i,j,k,M} = c_{i,r,k,M} \; \forall i \in \mathcal{I}, j \in \mathcal{J}_2, k \in \mathcal{K}, l \in \mathcal{L} \quad (9)$$

$$\sum_l q_{rd,k,l} = q_{re,k+1,M} \; \forall k \in \mathcal{K} \setminus N, l \in \mathcal{L} \quad (10)$$

$$c_{i,rd,k,l} = c_{i,re,k+1,M} \; \forall i \in \mathcal{I}, k \in \mathcal{K} \; N, l \in \mathcal{L} \quad (11)$$

$$q_{rd,N,l} = 0 \; \forall l \in \mathcal{L} \quad (12)$$

$$q_{re,1,M} = 0 \quad (13)$$

$$q_{re,k,M} = 0 \; \forall k \in \mathcal{K} \setminus 1 \text{ (optional)} \quad (14)$$

$$q_{sf,k,l+1} = q_{r,k,l} \; \forall k \in \mathcal{K}, l \in \mathcal{L} \setminus M \quad (15)$$

$$q_{sf,1,1} = 0 \quad (16)$$

$$c_{i,sf,k,l+1} = c_{i,r,k,l} \; \forall i \in \mathcal{I}, k \in \mathcal{K}, l \in \mathcal{L} \setminus M \quad (17)$$

$$q_{sf,k+1,1} = q_{p,k,M} \; \forall k \in \mathcal{K} \setminus N \quad (18)$$

$$c_{i,sf,k+1,1} = c_{i,p,k,M} \; \forall i \in \mathcal{I}, k \in \mathcal{K} \setminus N \quad (19)$$

$$q_{sf,1,1} = 0 \quad (20)$$

$$q_{p,k,l+1} = q_{fl,k,l+1} + q_{p,k,l} \forall k \in \mathcal{K}, l \in \mathcal{L} \setminus M \quad (21)$$

$$q_{p,k,l+1} \times c_{i,p,k,l+1} = q_{fl,k,l+1} \times c_{i,fl,k,l+1} + q_{p,k,l} \times c_{i,p,k,l} \quad (22)$$
$$\forall i \in \mathcal{I}, k \in \mathcal{K}, l \in \mathcal{L} \; M$$

$$q_{p,k,1} = q_{fl,k,1} \forall k \in \mathcal{K} \quad (23)$$

$$c_{i,p,k,1} = c_{i,fl,k,1} \forall i \in \mathcal{I}, k \in \mathcal{K} \quad (24)$$

In the material balance equations, q indicates flow (m^3/s), and c indicates the concentration (kg/m^3), and are model variables in the optimization problem. Q and C are the system input flow and concentration, and thereby inputs to the optimization problem. For the case study, we considered a *ff* flow of 100.2 (m^3/s) containing 1.7 (kg/m^3) of Li and 17 (kg/m^3) of Co along with *fd* flow of 120.1 (m^3/s) with 0.1 (kg/m^3) of Li and 0.2 (kg/m^3) of Co. Eqs. (1) to (3) specify the inputs to the cascade diafiltration system. Eq. (1) allow streams *ff* and *fd* to be injected at any point in the cascade. Eqs. (4) and (5) model the inlet mixer to each element, while (6) and (7) model the feed side finite element of a membrane stage. A splitter is used at the end of every stage to divide the retentate into product and recycle streams, governed by (8) and (9). Eqs. (10) to (14) model recycle between successive stages. Eq. (14) is an optional constraint that is used to analyze the cascade configuration without recycle. Connectivity between elements of the same stage on the feed side is modeled using (15) to (17) by linking the retentate and secondary feed streams. Cascading between stages is realized by allowing the permeate out of the last element to enter as secondary feed to the first element of the next stage, using (18) to (20). Eqs. (21) to (24) model the material balances on the permeate side of the stage. Flow streams that cannot be physically realized are set to 0. For example, (12) arises from the fact that in our present configuration, there can be no recycle streams as inlet to the last membrane stage.

Membrane transport phenomena:

$$q_{fl,k,l} = \frac{J_W \times L_k \times W}{M} \; \forall k \in \mathcal{K}, l \in \mathcal{L} \quad (25)$$

$$log\left(c_{i,r,k,l}\right) + (\alpha_i - 1) \times log\left(q_{f,k,l}\right) = log\left(c_{i,f,k,l}\right) + (\alpha_i - 1) \times log\left(q_{r,k,l}\right) \quad (26)$$
$$\forall i \in \mathcal{I}, k \in \mathcal{K}, l \in \mathcal{L}$$

Transport characteristics of the membrane are derived from first principle differential material balances. Eq. (25) governs the flux across the membrane, and (26) captures the concentration profile in the system. A log transformation is used in (26) to improve numeric conditioning. In the above equations, J_W is the specific flux across the membrane ($\frac{m^3}{m^2\,s}$), L and W denote the length and width of a membrane element (m), while α is the dimensionless membrane separation factor parameter. For the optimization problem, J_W, W, α_1(separation factor for Li) and α_2 (separation factor for Co) were held constant at 1.2 $\frac{m^3}{m^2\,s}$, 1.5 m, 1.3 and 0.5, respectively. Additionally, the height of the membrane channel (H) was fixed at 1.2 m, while the length of the membrane was a decision variable in the problem, thus enabling optimization of membrane area.

Purity and recovery of products:

$$R_p = \frac{q_{p,N,M} \times c_{1,p,N,M}}{Q_{ff} \times C_{1,ff} + Q_{fd} \times C_{1,fd}} \quad (27)$$

$$\frac{\sum_j Q_j c_{i,j} - q_{p,N,M} \times c_{1,p,N,M}}{\sum_j Q_j - q_{p,N,M}} \leq \bar{c_1} \forall\, j \in \mathcal{J}_5 \quad (28)$$

$$R_r = \sum_j Q_j c_{2,j} - q_{p,N,M} \times c_{2,p,N,M} \forall\, j \in \mathcal{J}_5 \quad (29)$$

Our model tracks the purity and recovery of products as quantities of interest. Eq. (27) is the recovery of the permeate side product R_p (Li rich solution). Eq. (28) is the purity constraint, limiting Li in the retentate product which is rich in Co. We use the convention of overbars and underbars to indicate upper and lower bounds, respectively. The recovery of the retentate product R_r is modeled by (29).

Modeling both R_p as well as R_r gives us the freedom to maximize either the recovery of Li or Co by changing the objective function of the optimization problem. In the following case study, we chose to maximize the recovery of Co, which is the more valuable solute.

System dimensions:

$$\theta_k \times \sum_{j,l} q_{j,k,l} + q_{sf,k,1} = q_{p,k,M} \quad (30)$$

$$\forall\, j \in \mathcal{J}\ sf, k \in \mathcal{K}, l \in \mathcal{L}$$

$$\sum_k L_k \times W \times H = A_m \ \forall\, k \in \mathcal{K} \quad (31)$$

Stage cuts θ (dimensionless) are defined by (30). The bounds on the stage cuts (38) prevent any single membrane stage from becoming too large, which would result in subsequent stages of the cascade being starved of feed. Expression (31) is used to calculate the overall membrane area A_m (m²) across all stages required for a given process. This quantity is also bounded to a finite value (37).

Physical bounds:

$$0 \leq q_{j,k,l} \leq \bar{q}, \forall\, j \in \mathcal{J}_1, k \in \mathcal{K}, l \in \mathcal{L} \quad (32)$$

$$0 \leq q_{j,k,M} \leq \bar{q}, \forall\, j \in \mathcal{J}_2, k \in \mathcal{K} \quad (33)$$

$$0 \leq c_{i,j,k,l} \leq \bar{c}, \forall\, i \in \mathcal{I}, j \in \mathcal{J}_1, k \in \mathcal{K}, l \in \mathcal{L} \quad (34)$$

$$0 \leq c_{i,j,k,M} \leq \bar{c}, \forall\, i \in \mathcal{I}, j \in \mathcal{J}_2, k \in \mathcal{K} \quad (35)$$

$$\underline{L} \leq L_k \leq \bar{L}, \forall\, k \in \mathcal{K} \quad (36)$$

$$\underline{A_m} \leq A_m \leq \overline{A_m} \quad (37)$$

$$\underline{\theta} \leq \theta_k \leq \bar{\theta}, \forall\, k \in \mathcal{K} \quad (38)$$

$$R_p \geq \underline{R_p} \quad (39)$$

The bounds on the system ensure that any solution obtained is physically realizable. For instance, the bounds on the flows, (32) and (33), prevent high recirculation rates in the system, which would incur uneconomically high piping and pumping costs. As before, we use underbars and overbars to indicate lower and upper bounds, respectively. The bounds $\bar{q}$=550 (m³/s), $\bar{c}$=10 (kg/m³), $\underline{L}$=0.1 (m), $\bar{L}$=1000 (m), $\underline{A_m}$=0 (m²), $\overline{A_m}$=1000 (m²), $\underline{\theta}$=0.01, $\bar{\theta}$=0.99, and $\underline{R_p}$= 0.005 were used in the case study.

Optimization problem (OPT1):

max	Recovery retentate product	Eq (29)
s.t.	Material balances	Eq. (1) – (24)
	Transport phenomena	Eq. (25) – (26)
	Product purity and recovery	Eq. (27), (28)
	System dimensions	Eq. (30), (31)
	Physical bounds	Eq. (32) – (39)

Optimization problem (OPT1) is implemented in Julia (Bezanson et. al., 2017) using JuMP modeling package (Dunning et. al., 2017). All instances were solved using the Ipopt (Wächter & Biegler, 2006) and the MA27 linear solver (HSL, 2014). For sense of model size, a ten-stage, ten-element problem has 2070 variables with 1759 equality constraints and 1 inequality constraint. Ipopt reliably finds an optimal solution in less than 0.9 seconds. In a sensitivity analyses of 10 values of N (number of stages) and 120 values of $\bar{c_1}$ (purity), it took 116 minutes to solve 1200 independent instances of (OPT1) using 10 cores in parallel on a high-performance cluster with dual Intel Xeon processors (2.5 GHz) and 256 GB of memory per node. Results from this sensitivity analysis are shown in Figures 2 and 3.

Results and Discussion

The optimization framework is applied to maximize the recovery and purity of a Co rich buffer solution as the retentate side product from a continuous diafiltration membrane cascade in two case studies.

Case Study 1: Baseline and Material Property Targets

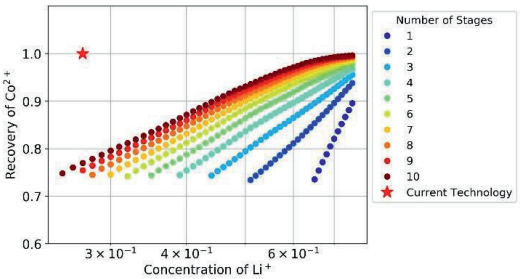

Figure 2: Sensitivity analysis results showing trade-offs between number of stages (N) and Li in the retentate (Co rich) product for a membrane with $\boldsymbol{\alpha_{Li} = 1.3}$.

We first characterize the trade-offs between retentate product purity and Co recovery using a membrane with Li separation factor of 1.3, which is comparable to values

reported by Armstrong et. al., (2013) and Qu et. al., (2015). Figure 2 shows the results of resolving (OPT1) for N=1 to N=10 stages and retentate purity limit of $\bar{c_1}$ =0.001 (kg/m³) to $\bar{c_1}$ =0.75 (kg/m³) Li. Because this is a binary separation, imposing an upper bound on Li concentration is equivalent to a lower bound on Co concentration. For a given purity, increasing the number of stages significantly increases the Co (product of interest) recovery. However, the results also show that the material under consideration does not possess the properties required to replace existing technologies in LIB recycling, such as Zhang et. al. (1998) which is marked with a red star in Figures 2 and 3. Efforts in developing novel membrane materials should be directed to shifting the curves in Figure 2 toward the red star, i.e. into the ***target design space***.

Case Study 2: Higher Performance Materials

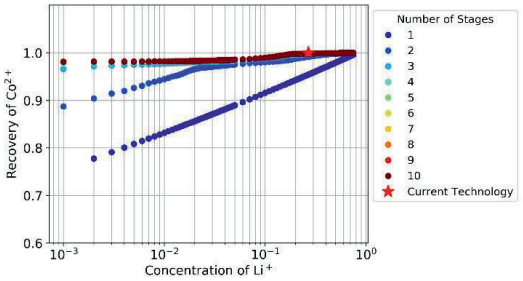

Figure 3: Sensitivity analysis for $\alpha_{Li} = 13$ membrane material. The performance curves for N=4 to N=10 overlap.

Next, we consider a membrane with a 10-fold larger Li permeability. We note that White et. al., (2016) and Zhu et. al., (2017) both report Li/Co selectivities greater than 1000, thus $\alpha_{Li} = 13$ is very reasonable. Figure 3 shows results from repeating the sensitivity analysis. With this modest increase in material performance, we predict a three-stage diafiltration membrane cascade is competitive with existing technology to concentrate the buffer solutions from LIB recycling. This is consistent with engineering intuition: increasing membrane permeability to Li increases its permeation through the membrane, more efficiently separating Li from Co in the feed solution, which results in a higher purity and recovery of Co in the retentate product. Moreover, the performance curves for N=4 to N=10 systems overlap in Figure 3, suggesting limited benefits from complex, many-stage designs. We also predict a carefully designed diafiltration cascade can achieve a 100-fold reduction in Li contamination with minimal impact on recovery compared to existing technologies. We highlight this superior performance is not possible with a one- or two-stage membrane, which underscores the importance of systems modeling and superstructure optimization. Experimental characterization of only a two-stage configuration such as done in Nambiar et. al. (2018) would likely miss this opportunity.

Figure 4 shows the optimum configuration for a 3-stage system with the higher Li permeability membrane ($\alpha_{Li} = 13$). In this system design, all of the feed is injected near the middle of the first membrane stage, and all of the dialysate in added to the beginning of that last stage. Co rich product is withdrawn almost entirely (97.6% of total Co rich product) from the retentate side of the first stage, with the rest coming from the second stage. 96.3% of the retentate from the second stage and all the retentate from the third stage are recycled as dialysate to the preceding stage.

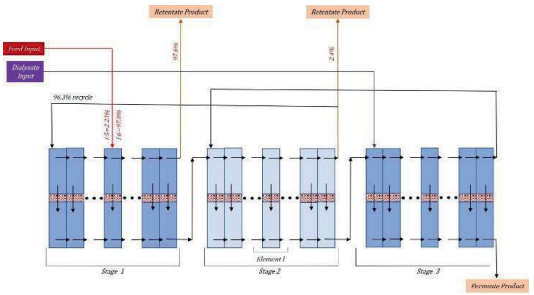

Figure 4: Optimum configuration for a 3-stage system that achieves 99.72% recovery of Co with Li concentration (impurity) of 0.27 (kg/m³)

Conclusions and Future Work

We propose a novel superstructure optimization framework to analyze and design multistage continuous diafiltration membrane cascades. Motivated by recent demand for energy storage technologies, we consider binary separation of lithium (Li) and cobalt (Co) ions for lithium ion battery recycling (LIB) as an example. Through sensitivity analysis, we determine material property goals (target values for Li selective) that could enable optimally designed 3-stage diafiltration cascades to outperform an existing LIB recycling technology.

We envision several extensions to fully realize a molecules-to-systems engineering framework that integrates predictive modeling, nanomaterial design, and lab-scale systems demonstrations. We plan to extend our model to incorporate both cost considerations and intricate mass transport mechanisms to better understand the underlying physics governing the process, and thereby design better materials. We seek to develop quantitative structure – property – processing relationships using data such as Rzayev (2005) and Weidman (2015). Such models would extend the superstructure optimization framework to consider material synthesis and processing, thereby offering systematic approach to inverse material design. We are also interested in parameter estimation and Bayesian inferential techniques to enable high-throughput characterization of novel membrane materials using dynamic data from simple

laboratory experiments. Finally, this application further motivates many outstanding computational challenges at the intersection of multiscale modeling, uncertainty quantification, and stochastic optimization for inverse design of membrane materials and associated systems, which we plan to explore.

Acknowledgments

We thank the University of Notre Dame for financial support as well as the ND Center for Research Computing for access to the HPC cluster used in this work.

References

Alnouri, S. Y., & Linke, P. (2014). Optimal seawater reverse osmosis network design considering product water boron specifications. *Desalination, 345, 112-127.*

Armstrong, J. A., Bernal, E. E. L., Yaroshchuk, A., & Bruening, M. L. (2013). Separation of ions using polyelectrolyte-modified nanoporous track-etched membranes. *Langmuir, 29(32), 10287–10296.*

Bezanson, J., Edelman, A., Karpinski, S., & Shah, V.B. (2017*)*. Julia: A fresh approach to numerical computing. *SIAM Review, 59(1), 65-98.*

Chen, Q., & Grossmann, I. E. (2017). Recent Developments and Challenges in Optimization-Based Process Synthesis. *Annual Review of Chemical and Biomolecular Engineering, 8(1), 249–283.*

Cheryan, M. (1998). *Ultrafiltration and Microfiltration Handbook. Taylor & Francis Routledge.*

Cremaschi, S. (2015). A perspective on process synthesis: challenges and prospects. *Computers & Chemical Engineering, 81, 130-137*.

Du, Y., Xie, L., Liu, Y., Zhang, S., & Xu, Y. (2015). Optimization of reverse osmosis networks with split partial second pass design. *Desalination, 365, 365-380.*

Du, Y., Liu, Y., Zhang, S., & Xu, Y. (2016). Optimization of seawater reverse osmosis desalination networks with permeate split design considering boron removal. *Industrial and Engineering Chemistry Research, 55, 12860-12879.*

Dunning, I., Huchette, J., & Lubin, M. (2017). JuMP: A modeling language for mathematical optimization. *SIAM Review, 59(2), 295-320*.

HSL. (2014). A collection of Fortran codes for large scale scientific computation. http://www.hsl.rl.ac.uk/

Khor, C. S., Foo, D. C. Y., El-Halwagi, M. M., Tan, R. R., & Shah, N. (2011). A superstructure optimization approach for membrane separation-based water regeneration network synthesis with detailed nonlinear mechanistic reverse osmosis model. *Industrial and Engineering Chemistry Research, 50, 13444-13456.*

Kotb, H., Amer, E. H., & Ibrahim, K. A. (2016). On the optimization of RO (Reverse Osmosis) system arrangements and their operating conditions. *Energy*, *103, 127-150*.

Lipnizki, F., Boelsmand, J., & Madsen, R. F. (2002). Concepts of industrial-scale diafiltration systems. *Desalination, 144(1–3), 179–184.*

Madsen, R. F. (2001). Design of sanitary and sterile UF-and diafiltration plants. *Separation and Purification Technology, 22–23, 79–87.*

Mulder, M. (1998). Basic Principles of Membrane Technology.

Nambiar, A. M. K., Li, Y., & Zydney, A. L. (2018). Countercurrent staged diafiltration for formulation of high value proteins. *Biotechnology and Bioengineering, 115(1), 139–144.*

Qu, S., Dilenschneider, T., & Phillip, W. A. (2015). Preparation of Chemically-Tailored Copolymer Membranes with Tunable Ion Transport Properties. *ACS Applied Materials and Interfaces, 7, 19746-19754.*

Rzayev, J., & Hillmyer, M. A. (2005). Nanochannel array plastics with tailored surface chemistry. *Journal of the American Chemical Society, 127(38), 13373–13379.*

Saif, Y., & Almansoori, A. (2015). Synthesis of reverse osmosis desalination network under boron specifications. *Desalination, 371, 26-36.*

Sassi, K. M., & Mujtaba, I. M. (2013). MINLP based superstructure optimization for boron removal during desalination by reverse osmosis. *Journal of Membrane Science, 440, 29-39.*

Senthil, S., & Senthilmurugan, S. (2016). Reverse Osmosis-Pressure Retarded Osmosis hybrid system: Modelling, simulation and optimization. *Desalination, 389, 78-97.*

Strathmann, H. (1980). Selective removal of heavy metal ions from aqueous solutions by diafiltration of macromolecular complexes. *Separation Science and Technology, 15(4), 1135–1152.*

Tian, Y., Demirel, S. E., Hasan, M. F., & Pistikopoulos, E. N. (2018). An overview of process systems engineering approaches for process intensification: State of the art. *Chemical Engineering and Processing-Process Intensification*, *133, 160-210*.

Uppaluri, R. V. S., Linke, P., & Kokossis, A. C. (2004). Synthesis and Optimization of Gas Permeation Membrane Networks. *Industrial & Engineering Chemistry Research, 43, 4305-4322.*

Uppaluri, R. V. S., Smith, R., Linke, P., & Kokossis, A. C. (2006). On the simultaneous optimization of pressure and layout for gas permeation membrane systems. *Journal of Membrane Science, 280, 832-848.*

Wächter, A. & Biegler, L. T. (2006) On the implementation of an interior-point filter line-search algorithm for large-scale nonlinear programming. *Math. Prog.*, *106(1), 25-57*.

Weidman, J. L., Mulvenna, R. A., Boudouris, B. W., & Phillip, W. A. (2015). Nanostructured Membranes from Triblock Polymer Precursors as High Capacity Copper Adsorbents. *Langmuir, 31(40), 11113–11123.*

White, N., Misovich, M., Alemayehu, E., Yaroshchuk, A., & Bruening, M. L. (2016). Highly selective separations of multivalent and monovalent cations in electrodialysis through Nafion membranes coated with polyelectrolyte multilayers. *Polymer (United Kingdom), 103, 478–485.*

Zhang, P., Yokoyama, T., & Itabashi, O. (1998). Hydrometallurgical process for recovery of metal values from spent nickel-metal hydride secondary batteries. *Hydrometallurgy, 50(1), 61–75.*

Zhu, Y., Ahmad, M., Yang, L., Misovich, M., Yaroshchuk, A., & Bruening, M. L. (2017). Adsorption of polyelectrolyte multilayers imparts high monovalent/divalent cation selectivity to aliphatic polyamide cation-exchange membranes. *Journal of Membrane Science, 537(March), 177–185.*